

# ConFusion: Sensor Fusion for Complex Robotic Systems using Nonlinear Optimization

Timothy Sandy, Simon Kerscher and Jonas Buchli

**Abstract**—We present ConFusion, an open-source package for online sensor fusion for robotic applications. ConFusion is a modular framework for fusing measurements from many heterogeneous sensors within a moving horizon estimator. ConFusion offers greater flexibility in sensor fusion problem design than filtering-based systems and the ability to scale the online estimate quality with the available computing power. We demonstrate its performance in comparison to an iterated extended Kalman filter in visual-inertial tracking, and show its versatility through whole-body sensor fusion on a mobile manipulator.

## I. INTRODUCTION

Sensor fusion is a valuable tool in the roboticist’s toolbox. As the complexity and state dimensionality of robots increase, information from numerous sensors must be considered to determine the full state of the robot. While general methods for sensor fusion are well-established, the design and implementation of state estimators for complex robots is tedious, making it difficult to easily add or remove sensors or investigate alternative state representations. In this work, we look to develop a framework for online sensor fusion that can support a wide range of robots and sensors and provides the flexibility and modularity necessary to easily build and evaluate state estimators for complex robots.

This paper introduces ConFusion, an open-source C++ package for online sensor fusion. ConFusion implements a moving horizon estimator (MHE) to optimize over a sliding batch of states to generate high-accuracy estimates for use in real-time control systems. The effort required to implement a new sensor fusion problem is no more than would be required for an extended Kalman filter, but ConFusion’s use of nonlinear optimization provides more flexibility in terms of state estimator design and the ability leverage additional computing resources to improve estimate quality by optimizing over a larger batch of states. Our modular framework allows for the easy incorporation of new sensors and estimated parameters and the ability to easily run offline batch calibration problems using the same state and measurement models.

This paper is structured as follows. We discuss the relevant prior work in Section II and give our main contributions in Section III. We then present the theory of the underlying sensor fusion problem in Section IV. The software structure and features of ConFusion are explained in Section V. Experimental results using ConFusion for visual-inertial tracking and whole body state estimation of a mobile manipulator are

The authors are with the Agile & Dexterous Robotics Lab, ETH Zurich, Switzerland. {tsandy, kersimon, buchli.j}@ethz.ch

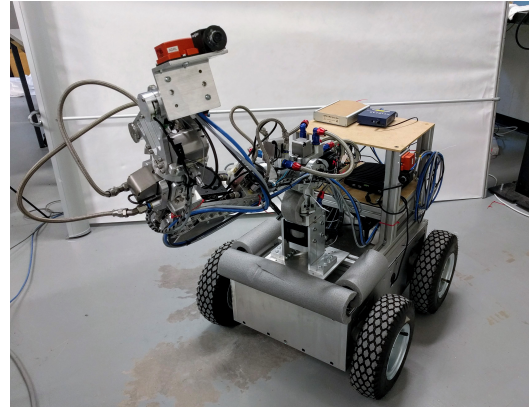


Fig. 1. IFmini, a hydraulically actuated manipulator on a skid-steer base, equipped with a camera and IMU mounted both on the base and the end-effector.

presented in Section VI. Finally, conclusions and an outlook to future work is given in Section VII.

## II. PRIOR WORK

Most robotic systems today use filter-based sensor fusion algorithms for generating real-time state estimates for use in motion control. Extended Kalman filters (EKF) are popular for their very low computational overhead, low memory requirements, and ease of implementation [1], [2], [3], [4]. In systems where non-linearities and non-uniform noise distributions are more dominant, other types of filters like the unscented Kalman filter (UKF) and particle filter are often used [5], [6]. Filter-based sensor fusion has multiple well-known weaknesses, though. The sequential process-then-update nature of filtering schemes places restrictions on the structure of the sensing system, since the use of an explicit process model, which models the evolution of the complete state from one time instance to the next, is required [7] and multiple and asynchronous process measurements cannot be directly incorporated. Additionally, since all measurements are processed sequentially, with the information provided by each measurement summarized by its immediate update to the state, estimate errors can bias the influence of future measurements and future measurements cannot be used to retrospectively improve the accuracy of past estimates.

More complex sensor fusion schemes facilitate the improvement of estimates after future measurements have been received. Fixed-lag smoothers achieve this by iteratively taking forward and backward recursive passes over a batch of states which slides over time. Fixed-lag smoothers still

enforce the restrictions in sensing system structure mentioned above, however. MHEs maintain an active batch of estimated states whose parameters are optimized simultaneously at each time-step. This allows the estimate of the state at a certain time to be repeatedly improved as the state marches back through the estimated batch of states. MHEs have been previously shown to outperform EKFs in monocular SLAM [8] and in monitoring chemical processes [9]. In a previous work, we showed that they can also provide smoother predictive estimates for use in high-frequency real-time robot controllers [10]. In [7], the two-state implicit filter is proposed to relax the sensing system design constraints imposed by filter-based approaches. The proposed filter is very similar to a MHE with a batch size of two, though updates to the estimated parameters are obtained using a recursive-style solver with less flexibility than the solvers used in MHEs. In [11], an open source MHE implementation is presented that was developed to maximize computational efficiency through automatic code generation and the use of specialized solvers. It was developed for applications with limited computational resources and it is not clear how effective it would be for use in complex robotic systems. It also does not provide the full flexibility of MHEs because it runs an EKF at the front of the optimized batch of states to perform marginalization.

The biggest downside of using MHEs for online state estimation is their large computational cost. Over the last 10 years, multiple open-source packages for non-linear-least-squares optimization have been developed to support bundle adjustment and simultaneous localization and mapping (SLAM) applications [12], [13]. While these solvers were not developed with online usage in mind, their scalability and computational efficiency make them valuable tools in online applications as well. Okvis is a point-feature-based online visual-inertial odometry system that uses the Ceres Solver [13] for non-linear-least-squares optimization in a MHE [14]. The sensor fusion algorithm employed is very similar to the one presented here, though we generalize the interface to support the fusion of an arbitrary number of general sensors and process models. iSAM2, also designed for SLAM applications, takes a different approach and estimates the full state history over time by efficiently factoring the probabilistic constraints between estimated parameters as they are induced by measurements over time [15]. While this method works well in SLAM problems, where links between states and landmarks are relatively sparse, it is not clear how it would transfer to more general sensor fusion problems for robot state estimation, where links between states and other estimated parameters are often persistent.

### III. CONTRIBUTIONS

The main contributions of this work are as follows. We present a general framework for online sensor fusion that allows for the easy incorporation of additional sensors, multiple non-synchronized process measurements, and which can leverage additional computing resources to improve estimate quality. Our C++ implementation is made available open-

source online<sup>1</sup>. Additionally, we demonstrate a novel state estimator for mobile manipulation using dual visual-inertial sensors at the robot's base and end-effector, showing that the additional sensors improve localization accuracy versus ground truth measurements.

### IV. MOVING-HORIZON ESTIMATION

We consider the problem of estimating the state of a robot at discrete instances of time ( $\mathbf{x}_t$ ) given a heterogeneous set of measurements. Measurements provide either information about the state of the robot at a specific time instance (such update measurements are written  $\hat{\mathbf{u}}_t$ ) or information relating the time evolution from one state instance to the next (a chain of such process measurements linking states  $\mathbf{x}_{t_i}$  and  $\mathbf{x}_{t_j}$  is written  $\hat{\mathbf{p}}_{t_i:t_j}$ ). In addition to the state of the robot, time-invariant (or static) parameters ( $\mathbf{s}$ ) are also estimated. These might be sensor intrinsic or extrinsic calibrations, or in the case of robot localization, the position of stationary references in the robot's environment. Update and process models of the following form are used to relate measurements received to the estimated parameters.

$$\begin{aligned} \mathbf{u}_t &= g(\mathbf{x}_t, \mathbf{s}) \\ \mathbf{x}_{t_j} &= h(\mathbf{x}_{t_i}, \mathbf{p}_{t_i:t_j}, \mathbf{s}) \end{aligned}$$

The  $f$  and  $g$  functions typically only involve a subset of the state and static parameters and can be non-linear in the estimated parameters and measurements. The Markov property is implicitly assumed, as process chains can only link successive states. Otherwise, no specific structure is assumed for these models, though the full observability of the estimated parameters is required from the full set of measurements and model considered to achieve good estimator performance.

Considering a batch of  $N$  states, determining the optimal set of parameters can be formulated as a least-squares problem of the following form.

$$\begin{aligned} \{\mathbf{x}_{t_0:t_N}^*, \mathbf{s}^*\} &= \arg \min_{\mathbf{x}_{t_0:t_N}, \mathbf{s}} \left[ \left\| \begin{bmatrix} \tilde{\mathbf{x}}_{t_0} - \mathbf{x}_{t_0} \\ \tilde{\mathbf{s}} - \mathbf{s} \end{bmatrix} \right\|_{W_M}^2 + \right. \\ &\quad \sum_{i=0}^N \left( \sum_{\hat{\mathbf{u}} \in \mathcal{U}_{t_i}} \|\hat{\mathbf{u}} - g(\mathbf{x}_{t_i}, \mathbf{s})\|_{W_{\hat{\mathbf{u}}}}^2 \right) + \\ &\quad \left. \sum_{i=1}^N \left( \sum_{\hat{\mathbf{p}} \in \mathcal{P}_{t_{i-1}:t_i}} \|\mathbf{x}_{t_i} - h(\mathbf{x}_{t_{i-1}}, \hat{\mathbf{p}}, \mathbf{s})\|_{W_{\hat{\mathbf{p}}}}^2 \right) \right] \end{aligned} \quad (1)$$

The first term in the function being minimized captures any prior knowledge about the initial value of the first state and static parameters ( $\tilde{\mathbf{x}}_{t_0}, \tilde{\mathbf{s}}$ ). We use the notation  $\|\mathbf{a}\|_B^2 = \mathbf{a}^T B \mathbf{a}$ . When assuming that uncertainty in the initial state and the noise in the update measurements are normally distributed, the weighting matrices of the prior knowledge and update measurement residuals are chosen to be the inverse covariance of those quantities. Assuming normally distributed process noise, the weighting for the

<sup>1</sup><https://bitbucket.org/tsandy/confusion>

process chain residuals is the inverse covariance of the state resulting from forward propagating the estimate of the preceding state (starting with no uncertainty on the preceding state) through the process measurements. With these choices for the weighting matrices, this sum-of-squares cost function is therefore made up of unit-less terms, each representing a probabilistic quantity. Although we use normal minus operators in the residual terms, in the presence of over-parameterized quantities (e.g. for rotational parameters) a distance function in the local tangent space should be used to compute these differences.

Equation (1) is solved iteratively using nonlinear least squares optimization. At each iteration, all of the residuals are linearized about the current value of the estimated parameters. If we define  $\mathbf{x}$  to be the a stacked vector of all of the estimated state and static parameters,  $\mathbf{e}_i = W^{\frac{1}{2}} f_i(\mathbf{x})$  such that  $\mathbf{e}_i^T \mathbf{e}_i = \|f_i(\mathbf{x})\|_W^2$ ,  $\mathbf{e} = [\mathbf{e}_0^T, \dots, \mathbf{e}_m^T]^T$ , and  $\mathbf{J} = \frac{\partial \mathbf{e}}{\partial \mathbf{x}}$ , the right side of (1) can be approximated as a linear least squares problem,

$$\arg \min_{\delta \mathbf{x}} \|\mathbf{J} \delta \mathbf{x} + \mathbf{e}\|^2, \quad (2)$$

where we now consider solving for the optimal increment to apply to the estimated parameters. When over-parameterized variables are being estimated,  $\delta \mathbf{x}$  is defined in the tangent space to the current estimate. By defining  $\mathbf{H} = \mathbf{J}^T \mathbf{J}$  and  $\mathbf{b} = -\mathbf{J}^T \mathbf{e}$ , solving (2) is equivalent to solving the so-called *normal equations* of the problem,  $\mathbf{H} \delta \mathbf{x} = \mathbf{b}$ . Since  $\mathbf{H}$  is inherently sparse due to the assumed Markov property, this equation is solved at each iteration using sparse Cholesky factorization. The Levenberg-Marquart algorithm is used to provide more robustness in optimization than the Gauss-Newton algorithm, but achieve convergence in fewer iterations than gradient descent [16]. Evaluating the individual residuals can be done in parallel, though solving the normal equations is done from a single thread.

In the presence of outlier measurements or non-normal noise distributions, the squared residual terms can be enclosed in a loss function (e.g. Huber loss) to decrease their influence in the presence of large residual values. This results in an iteratively re-weighted least squares problem.

### A. Marginalization

It is not feasible to solve (1) continuously online since the number of estimated parameters grows linearly over time. To deal with this, measurements are removed (or marginalized) out of the problem after some amount of time. The information contained in the marginalized measurements is approximated in what we call the prior constraint. This residual function relates the remaining estimated parameters which were linked to the marginalized measurements to their values at the time of marginalization. The MHE optimization problem considering a receding horizon (or batch) of  $N$

states is

$$\{\mathbf{x}_{t_i:t_{i+N}}^*, \mathbf{s}^*\} = \arg \min_{\mathbf{x}_{t_i:t_{i+N}}, \mathbf{s}} \|e_{prior}(\tilde{\mathbf{x}}_{t_i}, \mathbf{x}_{t_i}, \tilde{\mathbf{s}}, \mathbf{s})\|^2 + \sum_{j=i}^{i+N} \left( \sum_{\hat{\mathbf{u}} \in \mathcal{U}_{t_j}} \|\hat{\mathbf{u}} - g(\mathbf{x}_{t_j}, \mathbf{s})\|_{W_{\hat{\mathbf{u}}}}^2 \right) + \sum_{j=i}^{i+N} \left( \sum_{\hat{\mathbf{p}} \in \mathcal{P}_{t_{j-1}:t_j}} \|\mathbf{x}_{t_j} - h(\mathbf{x}_{t_{j-1}}, \hat{\mathbf{p}}, \mathbf{s})\|_{W_{\hat{\mathbf{p}}}}^2 \right). \quad (3)$$

Estimated parameters are marginalized out of the problem using block Gaussian elimination on the normal equations of the underlying least squares problem. To marginalize out some subset estimated parameters,  $\mathbf{x}_\mu$ , we first extract the portion of the problem that is directly dependent on  $\mathbf{x}_\mu$ . All cost functions which contain an element of  $\mathbf{x}_\mu$  are computed and linearized, generating the Jacobian of this sub-problem ( $\mathbf{J}_m$ ). All of the estimated parameters which appear in this sub-problem but are not being marginalized,  $\mathbf{x}_\lambda$ , will be constrained by the resulting prior constraint after marginalization. Once computed, the Jacobian of the sub-problem is reordered with  $\mathbf{x}_\mu$  in the left-most columns and the associated  $\mathbf{H}_m = \mathbf{J}_m^T \mathbf{J}_m$  is computed. The normal equations of the sub-problem can be written

$$\begin{bmatrix} \mathbf{H}_{\mu\mu} & \mathbf{H}_{\mu\lambda} \\ \mathbf{H}_{\lambda\mu} & \mathbf{H}_{\lambda\lambda} \end{bmatrix} \begin{bmatrix} \delta \mathbf{x}_\mu \\ \delta \mathbf{x}_\lambda \end{bmatrix} = \begin{bmatrix} \mathbf{b}_\mu \\ \mathbf{b}_\lambda \end{bmatrix}.$$

The Schur complement is taken to isolate  $\delta \mathbf{x}_\lambda$  as

$$\begin{bmatrix} \mathbf{H}_{\mu\mu} & \mathbf{H}_{\mu\lambda} \\ \mathbf{0} & \mathbf{H}^* \end{bmatrix} \begin{bmatrix} \delta \mathbf{x}_\mu \\ \delta \mathbf{x}_\lambda \end{bmatrix} = \begin{bmatrix} \mathbf{b}_\mu \\ \mathbf{b}^* \end{bmatrix}$$

where

$$\begin{aligned} \mathbf{H}^* &= \mathbf{H}_{\lambda\lambda} - \mathbf{H}_{\lambda\mu} \mathbf{H}_{\mu\mu}^{-1} \mathbf{H}_{\mu\lambda} \\ \mathbf{b}^* &= \mathbf{b}_\lambda - \mathbf{H}_{\lambda\mu} \mathbf{H}_{\mu\mu}^{-1} \mathbf{b}_\mu \end{aligned}$$

and  $\delta \mathbf{x}_\lambda$  can now be found independent of  $\delta \mathbf{x}_\mu$ .

The resulting prior constraint is formulated as

$$\mathbf{e}_p = \mathbf{J}_p(\tilde{\mathbf{x}}_\lambda - \mathbf{x}_\lambda) - (\mathbf{J}_p^T)^\dagger \mathbf{b}^*,$$

where  $\tilde{\mathbf{x}}_\lambda$  is the value of the remaining parameters linked to the prior sub-problem at the time of marginalization.  $\mathbf{J}_p$  is obtained from  $\mathbf{H}^* = \mathbf{J}_p^T \mathbf{J}_p$  via LU decomposition and  $(\mathbf{J}_p^T)^\dagger$  is computed using the Moore-penrose pseudo-inverse. When taking the Schur complement,  $\mathbf{H}_{\mu\mu}$  is inverted using Cholesky decomposition. While this marginalization scheme allows any estimated parameter to be marginalized from the problem at any time, our MHE implementation only considers the marginalization of one or more states at the front of the optimized batch of states. Static parameters can also be marginalized out when desired through an additional factorization step. The problem structure before and after marginalizing out a state is shown graphically in Fig. 2.

In the case that new static parameters are being continuously added to the problem over time, e.g. while performing SLAM in unknown environments, the prior constraint will

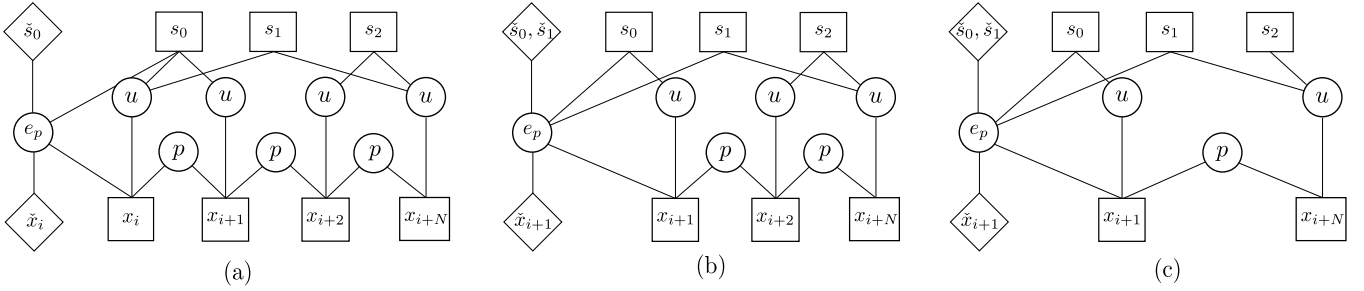


Fig. 2. Diagrams showing the transformation of an MHE due to marginalizing the first state (from a to b) and removing an intermediate state (b to c). Estimated parameters are drawn as squares, residuals as circles, and marginalized parameters as diamonds. Drawn edges represent the dependence of residuals on the connected parameters.

grow over time. To control the size of the prior constraint, static parameters can be removed from the prior constraint when desired. This is similarly done by applying the Schur complement to  $\mathbf{J}_p$ , but reordered such that the parameters to be removed appear in the left-most columns. As was done in our previous work in object-based SLAM [17], the parameters of the first state which are linked to the prior constraint can be similarly removed from the prior constraint to allow sensor fusion to be stopped and re-started while maintaining the accumulated relative certainties in the static parameters in a probabilistically consistent way.

### B. Removing Intermediate States

One of the main advantages of using a MHE for sensor fusion is that a state’s parameter estimates can be repeatedly refined considering measurements received later in time before the associated residuals are linearized about a marginalization point. It is therefore desirable that the batch of states being optimized span a large time horizon. Conventionally, that means that as big of a batch size as possible should be used, given the available computational resources. As we show in Section VI, it can be beneficial to periodically remove states before marginalization to allow a batch of a given size to span a longer time horizon.

It is straight-forward to remove states from the active batch before marginalization. The update measurements linked to the state being removed are simply dropped and the process chains linked to the preceding and following states are merged. This is shown pictorially in Fig. 2. The downside of removing states in this way is that the information contained in the dropped update measurements does not remain in the filter. This information was used however to counteract drift and improve the initialization and optimized value of the following state before it was dropped, however. It remains future work to investigate what strategies are the most effective for removing intermediate states. Initial experiments have shown that removing intermediate states at regular intervals is more effective than removing states based on some heuristic criteria (e.g. distance traveled between states) as those heuristics can potentially bias the generated estimates.

## V. SOFTWARE STRUCTURE

Our C++ implementation of the proposed MHE sensor fusion framework, called ConFusion, is made available open-source online <sup>2</sup>. ConFusion abstracts a sensor fusion problem into base classes representing the components of a MHE problem. To set up a sensor fusion problem the user should first create a derived version of *StateBase* which specifies the parameters that make up each instance of the state. The user must additionally define how the first state is initialized given an initial set of measurements and how new states are initialized from the previous state and a set of new measurements.

The user should implement measurement models for the update measurements and process chains used in the sensor fusion problem, inheriting from the *UpdateMeasurement* and *ProcessChain* base classes, respectively. We provide a set of measurement models, including our IMU process chain model, for re-use and encourage users to contribute new measurement models to build up a library of models over time.

All optimized parameters, whether as a part of the state or a static parameter are of type *Parameter*. Over-parameterized quantities can be assigned a local parameterization. A local parameterization is specified by  $\boxplus$  and  $\boxminus$  operations, which project estimates between global and local space. We provide parameter classes for quaternions and fixed-yaw orientations (for use in defining gravity-aligned reference frames) for general usage. All parameters can be configured to be optimized or constant at any time during operation simply by setting a flag.

To run a sensor fusion system online, measurements simply need to be passed into an instance of a *ConFusor*. Measurements can be arbitrarily delayed, even if they initially get assigned to older states in the active batch. Measurements can be added from one or more threads other than that which is running the estimator. The ConFusor provides functions to set up the MHE problem given new measurements, to run the optimizer, to marginalize desired leading states and static parameters, and to remove internal states. In this way, the user does not need to handle the creation of new states over

<sup>2</sup><https://bitbucket.org/tsandy/confusion>

time, and can control the removal of states without having to deal with the internal problem structure.

A class called the *BatchFusor* is additionally provided to run batch (or bundle adjustment) problems over a sequence of states, which were either cached while running ConFusion online or immediately created from a set of measurements. This can be used to periodically run offline calibration runs on longer trajectories where the observability of system calibration parameters is ensured.

ConFusion essentially wraps around the Ceres Solver [13] to support online sensor fusion. ConFusion was designed to expose the Ceres Solver API to the greatest extent possible so that the flexibility of Ceres can be leveraged by the user and so that users already familiar with the Ceres Solver can quickly get up and running. ConFusion therefore allows the user to utilize Ceres’ utilities for residual auto-differentiation, loss functions, and the wide range of solvers supported.

It is often difficult to debug sensor fusion systems because small implementation errors can cause the entire sensor fusion problem to quickly explode without a clear indication of what the cause was. For this reason, ConFusion provides some tools for diagnosing problems and analyzing system performance. Diagrams showing the links between parameters and residuals can be automatically generated, allowing the user to check that measurements are being linked to the expected parameters. Fig. 3 shows a diagram drawn by ConFusion for the mobile manipulator state estimator described in Section VI-B. ConFusion also comes with a general utility for data logging to allow users to easily store estimated parameter values and residuals over time for analysis.

## VI. EXPERIMENTS

We demonstrate the performance of ConFusion through two sets of experiments. First, we compare the performance of ConFusion to that of an iterated extended Kalman filter (IEKF) on the visual-inertial tracking of a sensor-head. Second, we show the extendability of ConFusion by performing whole-body sensor fusion on a mobile manipulator using visual and inertial sensors on both the base and end-effector of the robot and the manipulator kinematics. Our visual-inertial sensor heads are comprised of an Xsens MTI-100 inertial measurement unit (IMU), delivering accelerometer and gyroscope measurements at 400 Hz, and a PointGrey Blackfly monochrome camera providing images at 10 Hz and 5 mega-pixel resolution. As visual reference, we use stationary AprilTag [18] fiducial markers. Experiments were run on a standard laptop (Intel i7-4800MQ).

In both data-sets, we compare the estimated trajectories to ground truth measurements captured with a Leica Tracker, which provides full pose measurements of a tracked point at 50 Hz and with a nominal accuracy of less than 0.1 mm and 0.02 deg. One data-set was used to build a map of the fiducial markers and align the ground truth and sensor system coordinate frames and to align the trajectories in time. In order to maintain this alignment with the ground truth system, the data shown in this section was generated

	Pos Error (m)	Rot Error (rad)	Latency (sec)
IEKF	0.32	0.088	0.15
MHE, N=12	0.081	0.038	0.21
MHE, N=20	0.050	0.019	0.22
MHE, N=8, Drops	0.058	0.022	0.22

TABLE I  
ROOT-MEAN-SQUARED ACCURACY VERSUS GROUND TRUTH AND ESTIMATE LATENCY OF VISUAL-INERTIAL TRACKING FOR THE DATA SHOWN IN FIG. 4.

using the calibrated tag map as prior knowledge. Experiments showing the operation of the considered systems running online without the use of a prior tag map are included in the accompanying video<sup>3</sup>.

### A. Visual-Inertial Tracking

In this section, we show the performance of ConFusion in visual-inertial tracking. This analysis extends that from our previous work [10] to consider the case of tracking multiple tags and the impact batch size has on performance. The reader is referred to that paper for the sensor models and conventions employed here.

Fig. 4 shows the accuracy of the estimated IMU pose in the presence of aggressive motions using different sensor fusion schemes. In all cases, the generated estimates were forward-propagated through the more recent IMU measurements up to the time of the most recent IMU measurement to simulate the generation of real-time estimates. The latency of the first optimized estimates of the newest state in the MHE (or simply the estimated state for the IEKF) are shown in Table I. These latencies reflect the time required for image processing, sensor fusion computation and data transmission. In all cases, the MHE estimates are significantly more accurate than those of the IEKF, despite the additional latency of the MHE estimates. Three configurations for the MHE are shown. First, a batch size (N) of 12 was used. This was the maximum batch size which runs comfortably on one core of our CPU. A batch size of twenty was run using two CPU cores, and we can see that the MHE effectively leverages the additional computational power to improve the accuracy of the generated estimates. Finally, we ran the MHE with a batch size of 8 while dropping every second state after it was optimized the first time, as described in Section IV-B. This configuration could once again run on a single CPU core, though now the optimized batch spans a larger time horizon. We observe that this significantly improves performance with respect to the N=12 trial, approaching the accuracy obtained using two CPU cores.

### B. Mobile Manipulator Whole-Body State Estimation

We next consider the problem of estimating the state of a mobile manipulator. We use a new robot, called IFmini (Fig. 1), which consists of a 6 degree of freedom hydraulically actuated manipulator, designed and built by the

<sup>3</sup><https://youtu.be/Bhym83yP20Y>

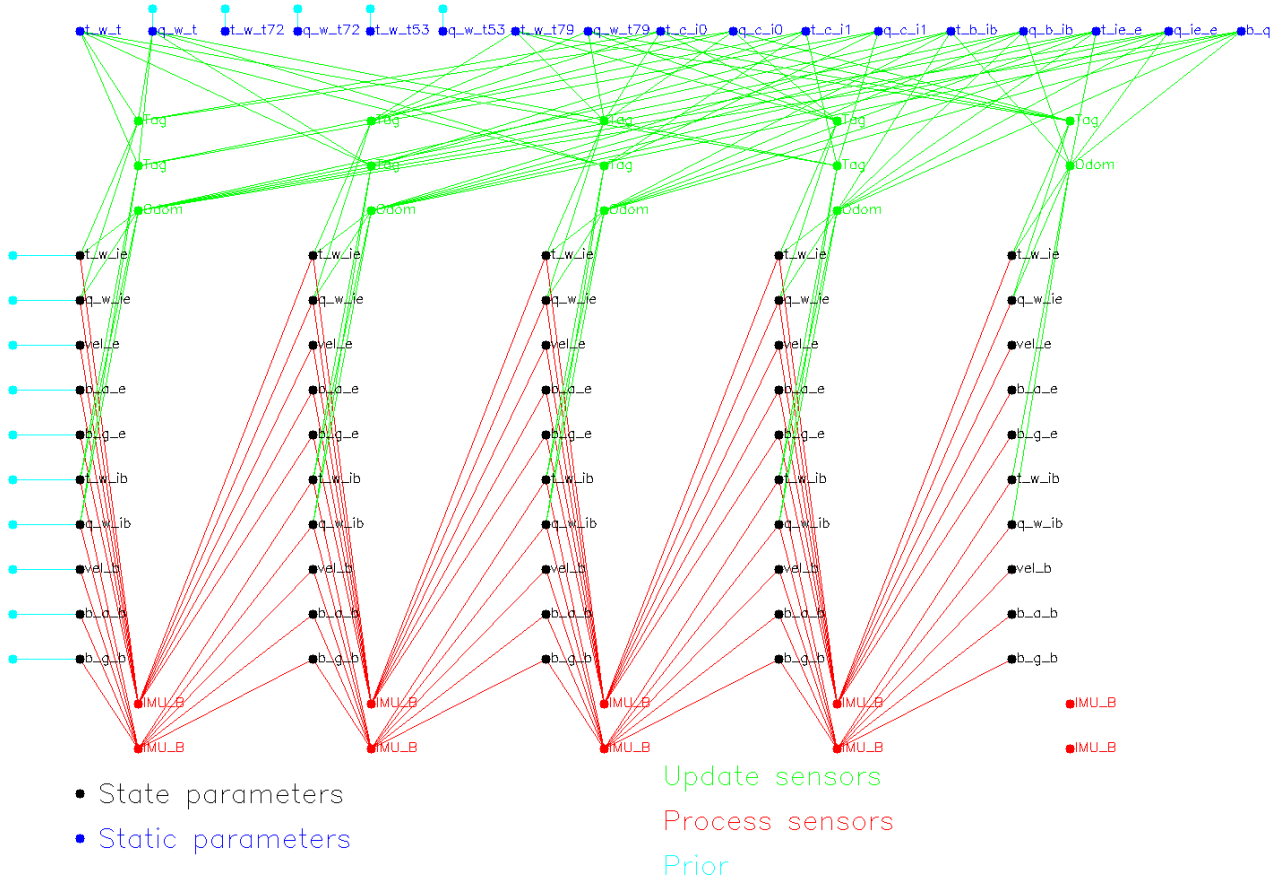


Fig. 3. Diagram showing a snapshot of the MHE problem solved for the IFmini state estimator (Section VI-B) with a batch size of 5. This diagram was automatically generated by ConFusion.

Italian Institute of Technology [19], mounted on top of a four-wheeled differential drive base, called the Supermega-bot by Inspectorbots. IFmini is a more dynamic, albeit smaller, successor to the In situ Fabricator (IF), designed for performing building construction tasks directly on the construction site [20].

In the interest of performing dynamic manipulation tasks with high accuracy, we would like to estimate the pose and velocity of IFmini’s end-effector within its environment. For use in control, these estimates should be available at high rate and with minimal latency. To support whole-body model-based control, it is desirable to additionally estimate the pose and velocity of the base. Here we show that we can generate accurate real-time estimates of the base and end-effector states using ConFusion. Building on our past results [10], the consistency of our MHE estimates allows for the accurate forward propagation of our state estimates through the IMU measurements up to real time for use in control.

In order to support whole-body sensor fusion, and also to evaluate which sensors are most valuable for generating high-accuracy real-time estimates, we have equipped IFmini with a camera and IMU on both the base and end-effector. In this configuration, the robot state is simply two times the state considered for visual-inertial tracking in the previous

section, with both cameras localizing the robot within the same map. We additionally fuse joint angle measurements and a model of the arm’s kinematics to relate the relative poses of the base and end-effector as an additional update measurement. The relative pose of the arm’s base frame with respect to the base IMU, the relative pose of the arm’s end-effector with respect to the end-effector IMU, and the joint angle biases for the middle four arm joints<sup>4</sup> are additionally used as static parameters to align the sensors with the arm kinematic model. Although ConFusion supports solving for these parameters online, we find that it is most effective to calibrate them separately in a batch problem and leave them fixed during online operation. This ensures that their values do not over-fit configuration-specific errors within the sensing system (e.g. camera intrinsic calibration error) while the robot is stationary.

Fig. 5 shows the end-effector pose real-time estimate error versus ground truth while undergoing whole body motions. Estimates were processed using different combinations of sensors, as shown in Table II. All estimates were generated using a batch size of 10 while throwing out every second

<sup>4</sup>Biases for the joints closest to the base and end-effector are not considered because they are compensated for in the relative poses of the IMUs with respect to the manipulator.

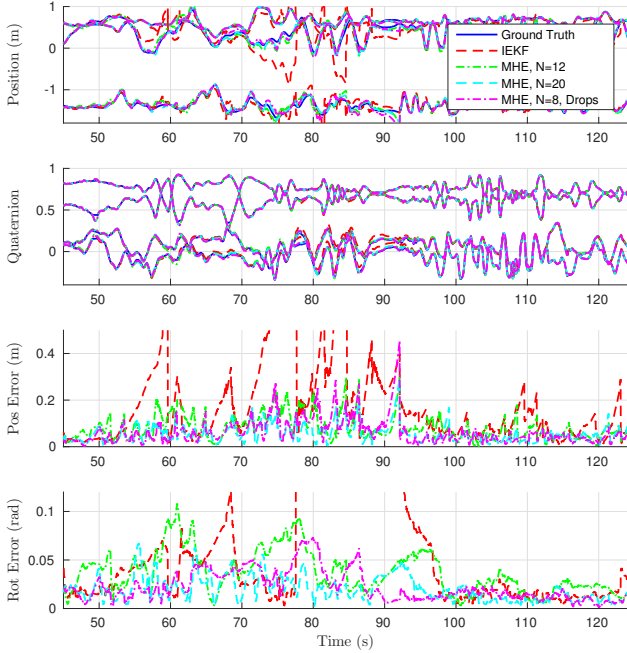


Fig. 4. Accuracy of the tracked sensor-head trajectories using different sensor fusion configurations, versus ground truth and in the presence of fast motion.

state after its first optimization. Once again, estimates were forward propagated up to the time of the most recent IMU measurement to simulate real-time operation on the robot. In these tests, estimates arrived with an average latency of 0.22 sec. The performance of the state estimator running on the robot in real-time is shown in the accompanying video<sup>5</sup>.

The flexibility of ConFusion allowed these different sensor configurations to be selected simply by changing an enumeration specifying which sensors were active. The same state representation could be used even though, in configuration 1, the entire base state was not estimated, and, in configuration 2, the base states have no linked process chain but are only linked to the rest of the problem through the update measurements and static parameters. This flexibility would not be possible in a filter-based framework.

We observe that the usage of the additional sensors on the base of the robot improves the estimator accuracy. With visual-inertial sensing on the end-effector alone, there are portions of the trajectory where no fiducials are visible (e.g. 28-30 sec), resulting in large errors due to uncorrected drift. Using the camera mounted on the robot base provides an additional viewpoint for viewing the fiducials, making it more likely that visual references are always seen. The use of the base camera and arm odometry also makes the extrinsic calibration of the cameras with respect to the manipulator and the joint angle biases immediately observable from the observation of the same reference in both cameras. Adding a second IMU on the base further improves estimator accuracy.

<sup>5</sup><https://youtu.be/Bhym83yP20Y>

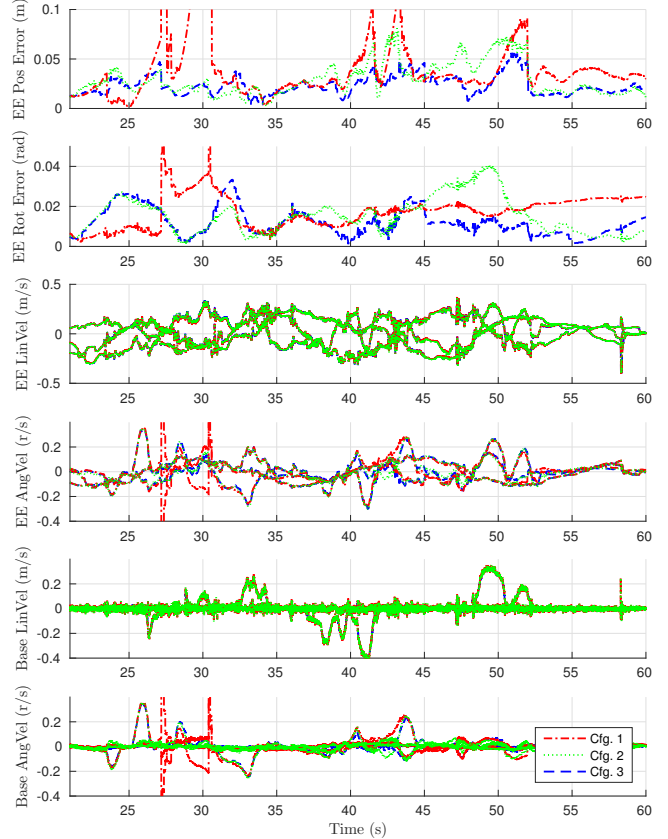


Fig. 5. IFmini end-effector pose estimate accuracy using different sets of sensors. Configuration 1 uses the end-effector camera and IMU. In this case, base estimates are generated by projecting the end-effector estimate to the base through joint odometry. Configuration 2 fuses those sensors plus the base camera and manipulator kinematic measurements. Configuration 3 additionally fuses the base IMU.

Since the base IMU constrains the evolution of the base portion of the state, it appears that its usage helps the system avoid over-fitting the base pose estimates to small camera calibration errors as observed fiducials move to different regions of the image plane.

## VII. CONCLUSION

In this paper, we have presented ConFusion, a general-purpose framework for online sensor fusion for robotic systems. We have demonstrated its ability to generate more accurate estimates than filtering-based approaches, leverage additional computing resources to improve estimator performance, and support complex sensor setups on mobile robots. As future work, we plan to investigate using more specialized nonlinear solvers that can better exploit the structure of the MHE problem and more principled strategies for determining which states should be removed from the estimator at which times. On the IFmini system, we plan to use the demonstrated state estimator to guide the execution of dynamic high-accuracy manipulation tasks and to investigate how the dual-camera setup can improve the localization performance within natural-feature-based SLAM maps.

Cfg.	EE Cam	EE IMU	Base Cam	Base IMU	Odometry	Pos [m]	Rot [rad]
1	X	X				0.047	0.018
2	X	X	X		X	0.026	0.014
3	X	X	X	X	X	0.021	0.011

TABLE II

THE SENSORS USED IN THE TESTS PLOTTED IN FIG. 5 ARE SHOWN, AS WELL AS THE ROOT-MEAN-SQUARED POSITION AND ROTATION ERRORS OVER THE PLOTTED INTERVAL.

#### ACKNOWLEDGEMENT

We would like to give special thanks to Prof. Andreas Wieser and Robert Presl for providing and operating the Leica Tracker for acquiring ground truth measurements. This research was supported by the Swiss National Science Foundation through the National Centre of Competence in Research Digital Fabrication (Agreement #51NF40.141853) and a Professorship Award to Jonas Buchli (Agreement #PP00P2\_138920).

#### REFERENCES

- [1] M. Li and A. I. Mourikis, "High-precision, consistent ekf-based visual-inertial odometry," *The International Journal of Robotics Research*, vol. 32, no. 6, pp. 690–711, 2013.
- [2] S. Lynen, M. W. Achtelik, S. Weiss, M. Chli, and R. Siegwart, "A robust and modular multi-sensor fusion approach applied to mav navigation," in *Intelligent Robots and Systems (IROS), 2013 IEEE/RSJ International Conference on*, pp. 3923–3929, IEEE, 2013.
- [3] M. Bloesch, M. Hutter, M. A. Hoepflinger, S. Leutenegger, C. Gehring, C. D. Remy, and R. Siegwart, "State estimation for legged robots-consistent fusion of leg kinematics and imu," *Robotics Science and Systems*, vol. 17, pp. 17–24, 2013.
- [4] X. Xinjilefu, S. Feng, W. Huang, and C. G. Atkeson, "Decoupled state estimation for humanoids using full-body dynamics," in *2014 IEEE International Conference on Robotics and Automation (ICRA)*, pp. 195–201, May 2014.
- [5] M. Bloesch, C. Gehring, P. Fankhauser, M. Hutter, M. A. Hoepflinger, and R. Siegwart, "State estimation for legged robots on unstable and slippery terrain," in *2013 IEEE/RSJ International Conference on Intelligent Robots and Systems*, pp. 6058–6064, Nov 2013.
- [6] M. F. Fallon, M. Antone, N. Roy, and S. Teller, "Drift-free humanoid state estimation fusing kinematic, inertial and lidar sensing," in *Humanoid Robots (Humanoids), 2014 14th IEEE-RAS International Conference on*, pp. 112–119, IEEE, 2014.
- [7] M. Bloesch, M. Burri, H. Sommer, R. Siegwart, and M. Hutter, "The two-state implicit filter recursive estimation for mobile robots," *IEEE Robotics and Automation Letters*, vol. 3, no. 1, pp. 573–580, 2018.
- [8] H. Strasdat, J. Montiel, and A. J. Davison, "Real-time monocular slam: Why filter?," in *Robotics and Automation (ICRA), 2010 IEEE International Conference on*, pp. 2657–2664, IEEE, 2010.
- [9] E. L. Haseltine and J. B. Rawlings, "Critical evaluation of extended kalman filtering and moving-horizon estimation," *Industrial & engineering chemistry research*, vol. 44, no. 8, pp. 2451–2460, 2005.
- [10] T. Sandy and J. Buchli, "Dynamically decoupling base and end-effector motion for mobile manipulation using visual-inertial sensing," in *2017 IEEE/RSJ International Conference on Intelligent Robots and Systems (IROS)*, pp. 6299–6306, Sept 2017.
- [11] M. Diehl, H. J. Ferreau, and N. Haverbeke, "Efficient numerical methods for nonlinear mpc and moving horizon estimation," in *Nonlinear model predictive control*, pp. 391–417, Springer, 2009.
- [12] R. Kümmerle, G. Grisetti, H. Strasdat, K. Konolige, and W. Burgard, "g 2 o: A general framework for graph optimization," in *Robotics and Automation (ICRA), 2011 IEEE International Conference on*, pp. 3607–3613, IEEE, 2011.
- [13] S. Agarwal and K. Mierle, "Ceres Solver." <http://ceres-solver.org>.
- [14] S. Leutenegger, S. Lynen, M. Bosse, R. Siegwart, and P. Furgale, "Keyframe-based visual-inertial odometry using nonlinear optimization," *The International Journal of Robotics Research*, vol. 34, no. 3, pp. 314–334, 2015.
- [15] M. Kaess, H. Johannsson, R. Roberts, V. Ila, J. J. Leonard, and F. Dellaert, "isam2: Incremental smoothing and mapping using the bayes tree," *The International Journal of Robotics Research*, vol. 31, no. 2, pp. 216–235, 2012.
- [16] T. D. Barfoot, *State Estimation for Robotics*. Cambridge University Press, 2017.
- [17] T. Sandy and J. Buchli, "Object-based visual-inertial tracking for additive fabrication," *IEEE Robotics and Automation Letters*, vol. 3, no. 3, pp. 1370–1377, 2018.
- [18] E. Olson, "AprilTag: A robust and flexible visual fiducial system," in *Proceedings of the IEEE International Conference on Robotics and Automation (ICRA)*, pp. 3400–3407, IEEE, May 2011.
- [19] B. U. Rehman, M. Focchi, M. Frigerio, J. Goldsmith, D. G. Caldwell, and C. Semini, "Design of a hydraulically actuated arm for a quadruped robot," in *International Conference on Climbing and Walking Robots (CLAWAR)*, 2015.
- [20] M. Gifthalder, T. Sandy, K. Dörfler, I. Brooks, M. Buckingham, G. Rey, M. Kohler, F. Gramazio, and J. Buchli, "Mobile robotic fabrication at 1:1 scale: the in situ fabricator," *Construction Robotics*, 2017.